

TECHNICAL ADVANCE

An *in vitro* system for the rapid functional characterization of genes involved in carotenoid biosynthesis and accumulation

Chao Bai¹, Sol M. Rivera², Vicente Medina¹, Rui Alves³, Ester Vilaprinyo³, Albert Sorribas³, Ramon Canela², Teresa Capell¹, Gerhard Sandmann⁴, Paul Christou^{1,5} and Changfu Zhu^{1,*}

¹Department of Plant Production and Forestry Science, School of Agrifood and Forestry Science and Engineering (ETSEA), University of Lleida Agrotecnio Center, Avenida Alcalde Rovira Roure 191, 25198, Lleida, Spain,

²Department of Chemistry, School of Agrifood and Forestry Science and Engineering (ETSEA), University of Lleida Agrotecnio Center, Avenida Alcalde Rovira Roure 191, 25198 Lleida, Spain,

³Department Ciències Mèdiques Bàsiques, Universitat de Lleida & Institut de Recerca Biomèdica de Lleida, Edifici Recerca Biomèdica I, Avenida Alcalde Rovira Roure 80, 25198 Lleida, Spain,

⁴Institute of Molecular Bioscience, J.W. Goethe University Frankfurt, Max von Laue Straße 9, 60438 Frankfurt, Germany, and

⁵Institució Catalana de Recerca i Estudis Avancats, Passeig Lluís Companys 23, 08010 Barcelona, Spain

Received 29 August 2013; revised 23 October 2013; accepted 11 November 2013; published online 23 November 2013.

*For correspondence (e-mail zhu@pvcf.udl.cat).

SUMMARY

We have developed an assay based on rice embryogenic callus for rapid functional characterization of metabolic genes. We validated the assay using a selection of well-characterized genes with known functions in the carotenoid biosynthesis pathway, allowing rapid visual screening of callus phenotypes based on tissue color. We then used the system to identify the functions of two uncharacterized genes: a chemically synthesized β -carotene ketolase gene optimized for maize codon usage, and a wild-type *Arabidopsis thaliana* ortholog of the cauliflower *Orange* gene. In contrast to previous reports (Lopez, A.B., Van Eck, J., Conlin, B.J., Paolillo, D.J., O'Neill, J. and Li, L. (2008) *J. Exp. Bot.* 59, 213–223; Lu, S., Van Eck, J., Zhou, X., Lopez, A.B., O'Halloran, D.M., Cosman, K.M., Conlin, B.J., Paolillo, D.J., Garvin, D.F., Vrebalov, J., Kochian, L.V., Kupper, H., Earle, E.D., Cao, J. and Li, L. (2006) *Plant Cell* 18, 3594–3605), we found that the wild-type *Orange* allele was sufficient to induce chromoplast differentiation. We also found that chromoplast differentiation was induced by increasing the availability of precursors and thus driving flux through the pathway, even in the absence of *Orange*. Remarkably, we found that diverse endosperm-specific promoters were highly active in rice callus despite their restricted activity in mature plants. Our callus system provides a unique opportunity to predict the effect of metabolic engineering in complex pathways, and provides a starting point for quantitative modeling and the rational design of engineering strategies using synthetic biology. We discuss the impact of our data on analysis and engineering of the carotenoid biosynthesis pathway.

Keywords: carotenoids, gene function, rice (*Oryza sativa*), 1-deoxy-D-xylulose 5-phosphate synthase, β -carotene ketolase, technical advance.

INTRODUCTION

The advent of large-scale DNA and RNA sequencing has provided unprecedented insights into the information content of plant genomes and transcriptomes (Ozsolak and Milos, 2011). However, the functions of many of the uncharacterized sequences remain unknown because annotations based on homology searching are only approximate, and the slow pace of conventional functional

characterization experiments has created a major information bottleneck (Zhu and Zhao, 2007).

Several large-scale direct functional annotation approaches have been developed, but these typically focus on single genes. For example, plant genes may be characterized rapidly by large-scale insertional mutagenesis using either transposons or T-DNA insertions (Myouga *et al.*,

2009), enhanced breeding approaches such as TILLING (Kurowska *et al.*, 2011), silencing approaches such as virus-induced gene silencing (VIGS; Purkayastha and Dasgupta, 2009) and RNA interference (RNAi; Purkayastha and Dasgupta, 2009), expression profiling using microarrays (Liu *et al.*, 2008), sequence census methods (RNA-seq; Ozsolak and Milos, 2011) or quantitative proteomics (Nikolov *et al.*, 2012), or by analysis of protein interactions using platforms such as the yeast two-hybrid system and its derivatives (Snyder and Gallagher, 2009). These approaches provide empirical functional data but the methods are indirect, i.e. function is inferred through expression profiles, loss-of-function phenotypes and associations with other gene products rather than direct biochemical analysis.

The drawbacks of *in silico* and empirical functional annotation have created significant challenges in characterization and engineering of plant metabolic pathways (Capell and Christou, 2004; Dafny-Yelin and Tzfira, 2007). Uncharacterized plant genes may be annotated on the basis of homology, but the assignments are often vague, e.g. a new sequence may be assigned as a cytochrome P450 mono-oxygenase, a glycosyltransferase or a methyltransferase, but this provides only a basic catalytic function without much information about substrate or product specificity. Similarly, a gene knockout or gene silencing experiment will show the overall impact of loss of function on plant metabolism and physiology, but there is no deeper insight into the role of the gene in metabolism. Yeast two-hybrid screens show potential interaction partners, but only if physical interactions occur. None of these methods, or any combination of them, completely joins the dots and shows the precise metabolic role of uncharacterized sequences, and how they fit into the surrounding context of known metabolic pathways.

We previously described a combinatorial gene transfer system that allows rapid analysis of metabolic genes in random combinations to provide insight into the roles of such genes, how they interact in the overall metabolic pathway, and the most optimum strategy to achieve synthesis of particular metabolic compounds (Zhu *et al.*, 2008; Farre *et al.*, 2013). This platform was established in maize (*Zea mays*) endosperm, which is most useful for assembling metabolic pathways that are relevant in seeds, such as those leading to the production of essential nutrients (Ramessar *et al.*, 2008; Zhu *et al.*, 2008). A more general platform for high-throughput functional analysis requires a less specific physiological structure and a shorter timescale than that provided by maize endosperm. Previous studies have shown that callus cultures in species such as maize, *Arabidopsis thaliana*, sweet potato (*Ipomoea batatas*), marigold (*Tagetes erecta*) and banana (*Musa acuminata*) may be used to test gene function (Paine *et al.*, 2005; Harada *et al.*, 2009; Kim *et al.*, 2011, 2013a,b; Vanegas-Espinoza *et al.*, 2011; Mlalazi *et al.*, 2012). However these studies

have been limited to single genes driven by a constitutive promoter because complex and time-consuming strategies are required to construct cassettes carrying multiple transgenes. This makes them unsuitable for the analysis of multiple gene interactions in complex metabolic pathways.

We hypothesized that our combinatorial transformation platform may be used to investigate multiple gene functions in rice (*Oryza sativa*) callus tissue, which may be prepared, transformed and screened much more rapidly than transgenic maize plants. Gene expression and protein accumulation in rice callus involves the same mechanisms that occur in the mature plant. Therefore, rice callus derived from zygotic embryos may be used as a surrogate platform for rapid analysis and evaluation of multiple candidate transgenes in a metabolic pathway to predict their behavior in whole plants.

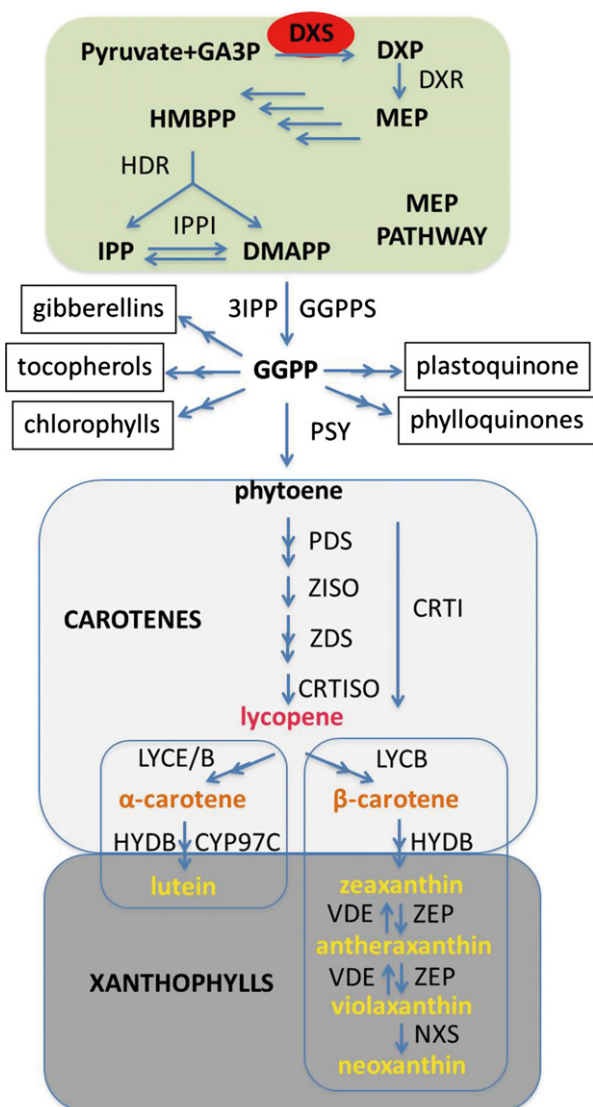
The approach was tested using well-characterized genes from the carotenoid biosynthesis pathway (Figure 1 and Figure S1; Zhu *et al.*, 2009, 2013; Ruiz-Sola and Rodriguez-Concepcion, 2012). Having confirmed that rice callus is suitable for the functional analysis of known genes, we then investigated the functions of a chemically synthesized uncharacterized β -carotene ketolase and an *Orange* ortholog, which could only be characterized by simultaneous expression of other genes from the carotenoid biosynthesis pathway in rice. The callus assay provides a rapid and inexpensive platform for functional characterization of uncharacterized genes by combinatorial expression, and may be combined with synthetic biology approaches for analysis of complex metabolic pathways and prediction of model-driven metabolic engineering strategies based on multigene expression (Zurbriggen *et al.*, 2012).

RESULTS

Combinatorial transformation of rice embryos with endosperm-specific carotenogenic transgenes generates rice callus lines that accumulate carotenoids

Embryo-derived rice callus is white in color and accumulates only minimal levels of carotenoids (Figures 2a and 3). Our analysis revealed the presence of small amounts of lutein and zeaxanthin in wild-type callus (Figure 3), which is similar to the carotenoid profile of white maize endosperm (Zhu *et al.*, 2008). This indicates that rice callus may likewise be used as a platform to test the combinatorial activity of multiple carotenogenic transgenes, but within a much shorter experimental time scale.

In pilot experiments to develop the platform, we transformed 7-day-old mature zygotic rice embryos with four constructs containing unlinked transgenes. These comprised the selectable marker *HPT* for hygromycin resistance, two carotenogenic transgenes with known functions in the committed carotenoid biosynthesis pathway, namely maize phytoene synthase 1 (*ZmPSY1*) and *Pantoea*



ananatis phytoene desaturase (*PaCRTI*), and the *A. thaliana* 1-deoxy-D-xylulose 5-phosphate synthase (*AtDXS*) gene, a limiting enzyme of the 2-C-methyl-D-erythritol 4-phosphate (MEP) pathway that supplies carotenoid precursors. The *HPT* gene was expressed constitutively, and expression of the three carotenogenic genes was driven by endosperm-specific promoters.

Remarkably, we observed during selection that the transgenic rice callus ranged in color from white through various shades of yellow to orange, representing expression of various combinations of the three carotenogenic transgenes and thus different carotenoid profiles (Figure 2a). Analysis of steady-state mRNA levels showed that *ZmPSY1* was expressed in all the yellow and orange callus lines but not in white callus which did not express *ZmPSY1* (even if the other carotenogenic transgenes were expressed), confirming that *ZmPSY1* is essential for carotenoid accumulation. Faint *ZmPSY1* hybridization bands in the white callus

Figure 1. The carotenoid biosynthesis pathway (Farre *et al.*, 2010, 2011).

All carotenoids are synthesized from the five-carbon monomeric building blocks isopentenyl diphosphate (IPP) and dimethylallyl diphosphate (DMAPP). Plastidial IPP is generated via the 2-C-methyl-D-erythritol 4-phosphate (MEP) pathway. The MEP pathway starts with glyceraldehyde-3-phosphate (GA3P) and pyruvate, which are converted into 1-deoxy-D-xylulose 5-phosphate (DXP) by DXP synthase (DXS). DXP reductoisomerase (DXR) converts DXP to MEP in the second step of the MEP pathway. MEP is then converted to 4-hydroxy-3-methylbut-2-enyl diphosphate (HMBPP) in four sequential reactions. Hydroxymethylbutenyl diphosphate reductase (HDR) simultaneously synthesizes IPP and DMAPP from HMBPP in the last step of the MEP pathway. Three IPP molecules are added to DMAPP to produce geranylgeranyl diphosphate (GGPP), which serves as the immediate precursor not only for carotenoids but also for biosynthesis of gibberellins and the side chain of chlorophylls, tocopherols, phyloquinones and plastoquinone. The first committed step in carotenoid biosynthesis is condensation of two molecules of GGPP by phytoene synthase (PSY) to produce phytoene. Phytoene is converted into all-*trans* lycopene by the action of two desaturases and two isomerases: phytoene desaturase (PDS), ζ -carotene isomerase (ZISO), ζ -carotene desaturase (ZDS) and carotenoid isomerase (CRTISO). The bacterial phytoene desaturase (CRTI) performs all the desaturation and isomerization reactions performed by plant PDS, ZISO, ZDS and CRTISO. As CRTI has low homology with plant PDS and ZDS, and reduces the number of transgenes required, it is widely used in metabolic engineering. Lycopene represents a branch in the pathway, leading to either α - or β -carotenes. In the α -carotene branch, addition of one ϵ -ring and one β -ring to lycopene by lycopene ϵ -cyclase (LYCE) and lycopene β -cyclase (LYCB), respectively, produces α -carotene. In the β -carotene branch, lycopene is cyclized to produce the provitamin A carotenoid γ -carotene and then β -carotene by addition of β -rings to both ends of the linear lycopene molecule by LYCB. β - and α -carotene are redundantly hydroxylated by non-heme di-iron β -carotene hydroxylases (BCH1 and BCH2) and cytochrome P450-type β - and ϵ -hydroxylases (CYP97A, CYP97B and CYP97C). β -xanthophylls are epoxidated and de-epoxidated by zeaxanthin epoxidase (ZEP) and violaxanthin de-epoxidase (VDE), respectively giving rise to the xanthophyll cycle.

samples represented the endogenous *OsPSY1* gene, which is expressed at minimal levels in rice callus. The appearance of color in the callus tissue confirmed that the 'endosperm-specific' wheat (*Triticum aestivum*) low-molecular-weight glutenin, barley (*Hordeum vulgare*)_D-hordein and rice prolamins promoters were each also active in dedifferentiated rice tissue, as previously reported for the maize 27 kDa γ -zein promoter (Wu and Messing, 2009).

We found a precise correlation between the phenotypes and expressed transgenes at the mRNA level (Figure 2a,b). Rice callus expressing *ZmPSY1* alone was pale yellow in color, whereas callus expressing both *ZmPSY1* and *AtDXS* was darker yellow and callus expressing both *ZmPSY1* and *PaCRTI* was yellow/orange. Callus expressing all three carotenogenic transgenes was a darker orange color. Therefore, we were able to make accurate predictions of the transgenes expressed in each callus line by simple visual screening, allowing straightforward selection of callus pieces for further experiments or regeneration into transgenic plants.

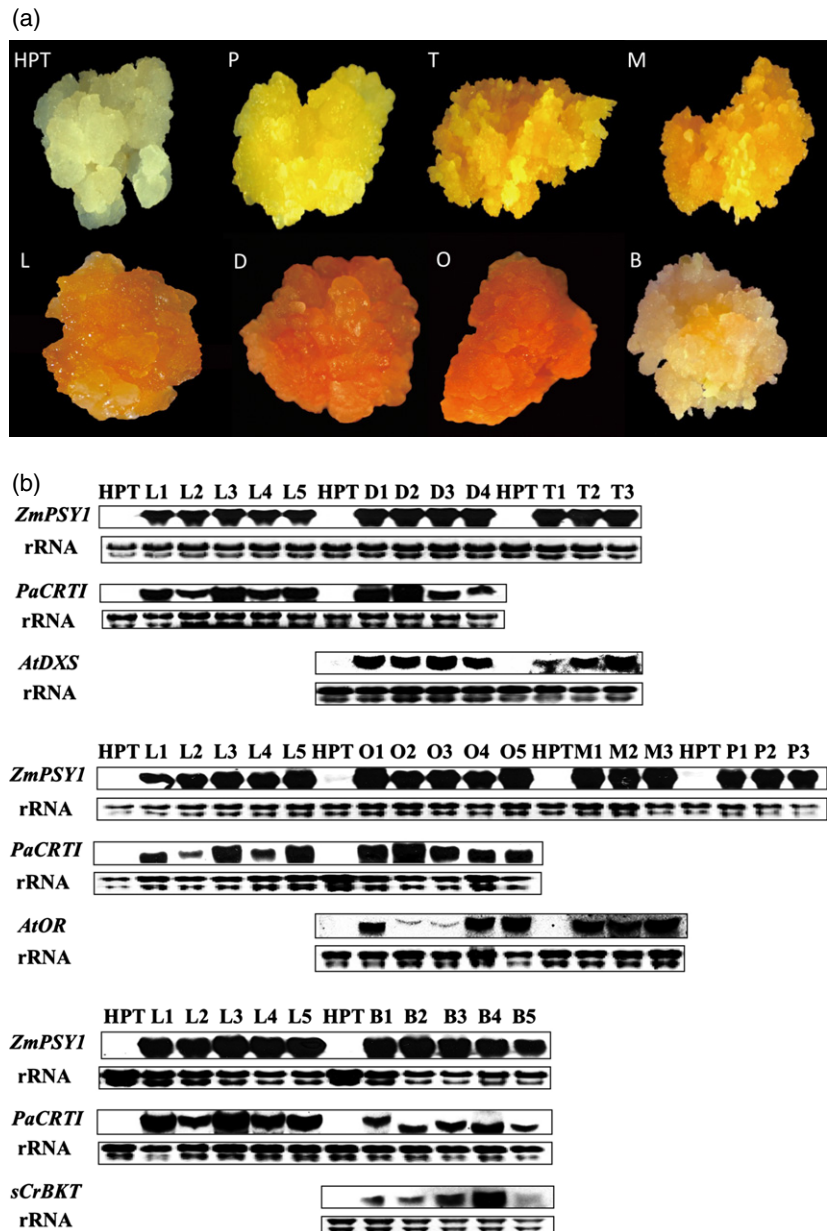
Metabolic profiling and mathematical modeling of transgenic callus lines reveals a correlation between transgene expression and carotenoid accumulation

Analysis of carotenoid content and composition by UHPLC showed that the various color phenotypes reflected

Figure 2. Phenotypes and genotypes of seven rice callus combinatorial transformants.

(a) Phenotypes of seven transgene combinations expressed in rice callus. HPT, callus expressing *HPT* (white color); P, expression of *ZmPSY1* alone results in a pale yellow color; expression of *ZmPSY1* and *AtDXS* in T, *ZmPSY1* and *AtOR* in M, and *ZmPSY1* and *PaCRTI* in L, result in a similar yellow color; expression of *AtDXS* in addition to *ZmPSY1* and *PaCRTI* in D, or in addition to *ZmPSY1*, *PaCRTI* and *AtOR* in O, results in a similar orange color; B, expression of *ZmPSY1*, *PaCRTI* and *sCrBKT* generates colors ranging from pink to red depending on the accumulation of ketocarotenoids.

(b) Analysis of mRNA transgenic rice callus (25 µg of total rRNA was loaded for each sample). Abbreviations: HPT, callus expressing *HPT*; L1–L5, transgenic callus expressing *ZmPSY1* and *PaCRTI*; D1–D4, transgenic callus expressing *AtDXS*, *ZmPSY1* and *PaCRTI*; T1–T3, transgenic callus expressing *ZmPSY1* and *AtDXS*; O1–O5, transgenic callus expressing *ZmPSY1*, *PaCRTI* and *AtOR*; M1–M3, transgenic callus expressing *ZmPSY1* and *AtOR*; P1–P3, transgenic callus expressing *ZmPSY1* alone; B1–B5, transgenic callus expressing *ZmPSY1*, *PaCRTI* and *sCrBKT*.



different metabolic profiles, confirming a direct correlation between the genotype and the metabolic phenotype of the callus lines. The white callus did not express *ZmPSY1* and contained similar levels of total carotenoids regardless of the additional transgene complement, i.e. control lines expressing *HPT* alone accumulated the same level of carotenoids as callus also expressing *PaCRTI* or *AtDXS* or both genes simultaneously. The yellow callus expressing *ZmPSY1* alone accumulated β -carotene and phytoene in similar amounts, as well as smaller amounts of α -carotene, lutein, violaxanthin and zeaxanthin (Figure 3, Figure S2 and Table S1). The darker yellow callus expressing *ZmPSY1* and *AtDXS* accumulated 1.8-fold more total carotenoids than callus expressing *ZmPSY1* alone, most of

which was β -carotene, whereas the levels of phytoene and the minor carotenoids hardly changed. The yellow/orange callus expressing *ZmPSY1* and *PaCRTI* accumulated twice as much total carotenoids than callus expressing *ZmPSY1* alone, but, although most of this was again β -carotene, the next most abundant carotenoid was α -carotene, which was three times more abundant than phytoene. Finally, the orange callus expressing all three transgenes accumulated 3.5-fold more total carotenoids than callus expressing *ZmPSY1* alone, again mostly β -carotene, α -carotene and phytoene in similar proportions to the *ZmPSY1*-*PaCRTI* callus, but also with significant amounts of lutein (Figure 3, Figure S2 and Table S1). The presence of *AtDXS* in addition to *ZmPSY1* and *PaCRTI* therefore increased the

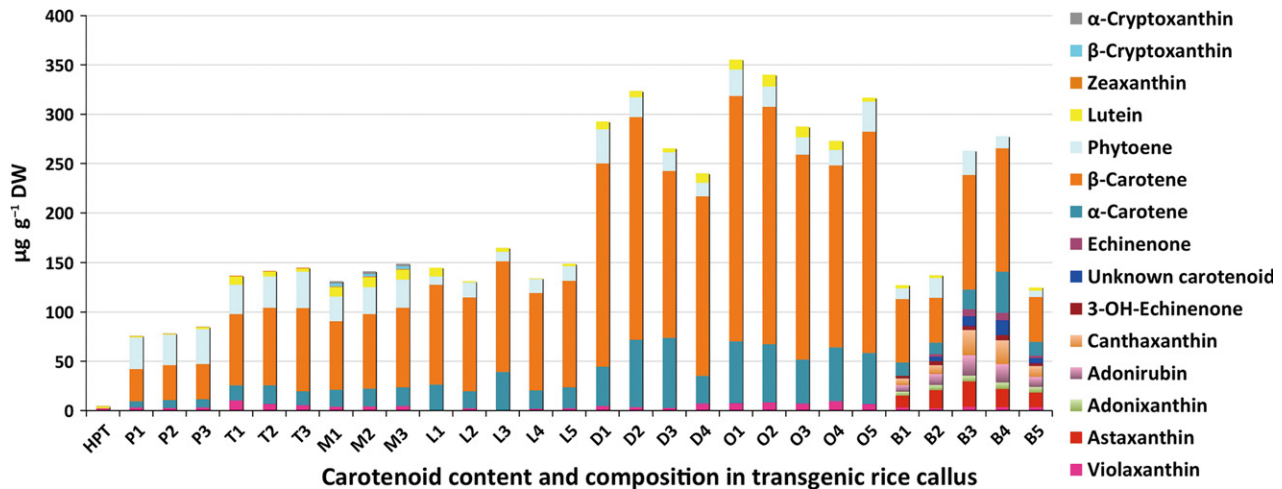


Figure 3. Carotenoid content and composition in transgenic rice callus. Carotenoid content and composition were analyzed by UHPLC. The various colored blocks represent different carotenoid compositions as indicated in the key. Values are means of three independent measurements. Column names are defined in the legend to Figure 2.

carotenoid content 1.9-fold, suggesting that the *A. thaliana* *DXS* gene boosts carotenoid biosynthesis by alleviating the limited supply of precursors into the pathway.

Although the transgene expression levels correlated with carotenoid accumulation (Figure 2a,b), this conclusion required the basic assumption that expression of each gene remained approximately constant among the various lines. In support of this assumption, quantification of mRNA in the Northern blots using ImageJ software (<http://rsb.info.nih.gov/ij/>) suggested that, for each transgene, the amount of expressed mRNA remained approximately constant in each transformed line (Figure 2b and Table S2). If we assume a constant rate of protein synthesis, the abundance of each protein should therefore be constant across the various callus lines also, and the metabolite concentrations should therefore allow us to model the behavior of carotenoid biosynthesis. We validated these assumptions experimentally as described below.

First, phytoene production appears to limit the production of downstream carotenoids. This may be inferred because transgenic callus expressing *ZmPSY1* increases the abundance of carotenoids 17-fold. Second, the quantity of phytoene precursors produced in the callus appears to limit the production of downstream carotenoids, even in the presence of *ZmPSY1*. This may be inferred because the *ZmPSY1-AtDXS* lines accumulate almost twice the level of total carotenoids present in the *ZmPSY1* lines. Third, endogenous carotene desaturase activity in rice appears to account for a significant proportion of carotenoid production from phytoene. This may be inferred because both the *ZmPSY1* and *ZmPSY1-AtDXS* lines produce 20–30-fold more carotenoids than control callus. However, this native activity may limit carotenoid production, because introducing the exogenous *CRTI* gene boosts carotene production

and reduces the amount of phytoene compared to lines that do not express *CRTI*.

In order to validate these hypotheses, we created simplified mathematical models of the callus system, and investigated whether the dynamic behavior of the models was consistent with the experimental data (Table S3). Figure S3 shows the simplified pathway that was modeled. The modeling process is described in Experimental Procedures and Method S1. Table S4 summarizes the parameter values for the models. We found that the models quantitatively reproduced what was observed in the transgenic lines.

The first hypothesis cannot be tested by the modeling process, as it represents a founding assumption for the modeling process itself. Analysis of the model parameters revealed that introducing *AtDXS* generates approximately twice the amount of flux per unit time to produce phytoene than callus lines lacking this transgene. This is consistent with the second hypothesis. In addition, the production of carotenoids in lines that lack *CRTI* may be explained by endogenous flux channels. This activity accounts for a significant amount of α -carotene and β -carotene production even in lines expressing *CRTI*, and is consistent with the third hypothesis. A more detailed analysis is presented in Method S1.

Functional characterization of a chemically synthesized, codon-optimized *Chlamydomonas reinhardtii* β -carotene ketolase gene

Having established the suitability of the callus platform for analysis of carotenogenic genes with known functions, we analyzed a synthetic *C. reinhardtii* β -carotene ketolase gene (*sCrBKT*), codon-optimized for cereals, controlled by an endosperm-specific promoter, in this case the γ -zein gene promoter from maize (GZ63).

We investigated the function of the chemically synthesized *sCrBKT* gene and the interaction of its product with other carotenogenic enzymes by transforming 7-day-old rice embryos with *ZmPSY1*, *PaCRTI* and *sCrBKT*. We recovered many independent callus lines under hygromycin selection, including a large proportion that were pink in color, suggesting accumulation of ketocarotenoids (Figure 2). This was confirmed by UHPLC analysis, which showed not only the presence of ketocarotenoids but also higher levels of β -carotene (Figure 3, Figure S2 and Table S1). The best-performing pink callus line contained $277.6 \pm 0.6 \mu\text{g g}^{-1}$ dry weight of total carotenoids, including $18.5 \pm 1.3 \mu\text{g g}^{-1}$ astaxanthin, $6.7 \pm 0.2 \mu\text{g g}^{-1}$ adonixanthin, $18.6 \pm 0.8 \mu\text{g g}^{-1}$ adonirubin, $24 \pm 1.8 \mu\text{g g}^{-1}$ canthaxanthin, $5.3 \pm 0.3 \mu\text{g g}^{-1}$ 3-OH-echinone, $7.5 \pm 1.2 \mu\text{g g}^{-1}$ echinenone, $15 \pm 2.7 \mu\text{g g}^{-1}$ unknown molecule, $124.6 \pm 3.8 \mu\text{g g}^{-1}$ β -carotene, $12.3 \pm 1.6 \mu\text{g g}^{-1}$ phytoene, $41.6 \pm 0.5 \mu\text{g g}^{-1}$ α -carotene and $3.3 \pm 0.04 \mu\text{g g}^{-1}$ violaxanthin. These data show that ketolation of β -carotene in combination with hydroxylation by the endogenous rice hydroxylase occurred due to the presence of *sCrBKT*, which is functional in transgenic rice callus, and that the maize 'endosperm-specific' γ -zein gene promoter (GZ63) is active in callus tissue, like the other endosperm-specific promoters used in the preceding experiments.

Functional characterization of the *Arabidopsis thaliana*

Orange gene

Another biological phenomenon that may be investigated using the callus platform is carotenoid accumulation in subcellular organelles. The cauliflower (*Brassica oleracea* var. *botrytis*) *Orange* gene (*OR*) is involved in this process by regulating the development of chromoplasts, which store carotenoids and accumulate large amounts of β -carotene. The cauliflower *OR* gene was identified as a gain-of-function mutant allele that accelerates the formation of chromoplasts, creating a metabolic sink for carotenoid accumulation. This allele also functions in a heterologous background (Lu *et al.*, 2006; Li and Van Eck, 2007; Lopez *et al.*, 2008). Recently, a sweet potato ortholog of *OR* was shown to promote accumulation of carotenoids by inducing expression of carotenoid biosynthesis genes in transgenic sweet potato callus (Kim *et al.*, 2013b).

We identified the *A. thaliana* *OR* gene (*AtOR*) by sequence comparison with the cauliflower ortholog, and used this sequence to test our callus platform in more detail. We cloned *AtOR* from *A. thaliana* leaf tissue by RT-PCR, and then introduced it into a plant expression vector under the control of the wheat low-molecular-weight glutenin gene promoter. We transformed rice embryos with *ZmPSY1*, *PaCRTI*, *AtOR* and *HPT*, generating a number of callus lines that were orange or yellow in color, whereas the control callus remained white (Figure 2a). The callus expressing additional *AtOR* to the gene complement

showed an increased carotenoid content (2.2-fold) compared with callus expressing *ZmPSY1* and *PaCRTI* (Table S1). Samples of the orange and yellow callus were analyzed by UHPLC. The best-performing orange callus was shown to express all the transgenes, and produced $355.3 \pm 70.6 \mu\text{g g}^{-1}$ dry weight of total carotenoids, comprising $248.1 \pm 46.4 \mu\text{g g}^{-1}$ β -carotene, $27.1 \pm 6.8 \mu\text{g g}^{-1}$ phytoene, $62.8 \pm 12.8 \mu\text{g g}^{-1}$ α -carotene, $10 \pm 2.9 \mu\text{g g}^{-1}$ lutein and $7.3 \pm 1.7 \mu\text{g g}^{-1}$ violaxanthin, confirming that the *AtOR* gene was functional and that was able to boost the accumulation of carotenoids in transgenic callus and particularly to enhance the accumulation of β -carotene (Figure 3, Figure S2 and Table S1).

Representative transgenic callus samples were examined by microscopy. Orange crystal-like structures were observed in the chromoplasts of orange callus samples expressing *OR* (Figure 4a), similar to those reported in transgenic plants expressing the cauliflower *OR* gene (Lu *et al.*, 2006; Lopez *et al.*, 2008). Interestingly, the same structures were observed in transgenic callus samples expressing *AtDXS* (Figure 4a). Transmission electron microscopy revealed numerous pigment-containing plastoglobuli that varied in size and electron density in both the *AtDXS* and *AtOR* transgenic lines (Figure 4b and Figure S4).

DISCUSSION

Rice callus provides a functional screening platform for carotenoid biosynthesis genes even if the genes are controlled by endosperm-specific promoters

We previously described a combinatorial gene transfer platform based on white maize endosperm for functional analysis of combinations of metabolic genes (Zhu *et al.*, 2008). The endosperm of M37W maize is white because the carotenoid biosynthesis pathway is blocked at the first committed step, providing a blank canvas for analysis of carotenogenic genes introduced by gene transfer, and further allowing rapid analysis of diverse genotypes by visual screening for endosperm color. The endosperm tissue may also be studied in more detail by UHPLC, allowing quantitative analysis of all carotenoids, and this means the platform may be extended to any other metabolic pathway that is also missing in endosperm tissue.

The usefulness of the maize platform in functional characterization of metabolic genes is constrained by the time needed to regenerate transgenic plants carrying combinations of transgenes. Other researchers have reported use of callus tissue from maize, *A. thaliana*, sweet potato, marigold and banana to characterize gene functions and expression levels, although only individual genes were tested in these cases (Paine *et al.*, 2005; Harada *et al.*, 2009; Kim *et al.*, 2011, 2013a,b; Vanegas-Espinoza *et al.*, 2011; Mlalazi *et al.*, 2012). We therefore adapted our combinatorial platform to work in rice callus, thus permitting

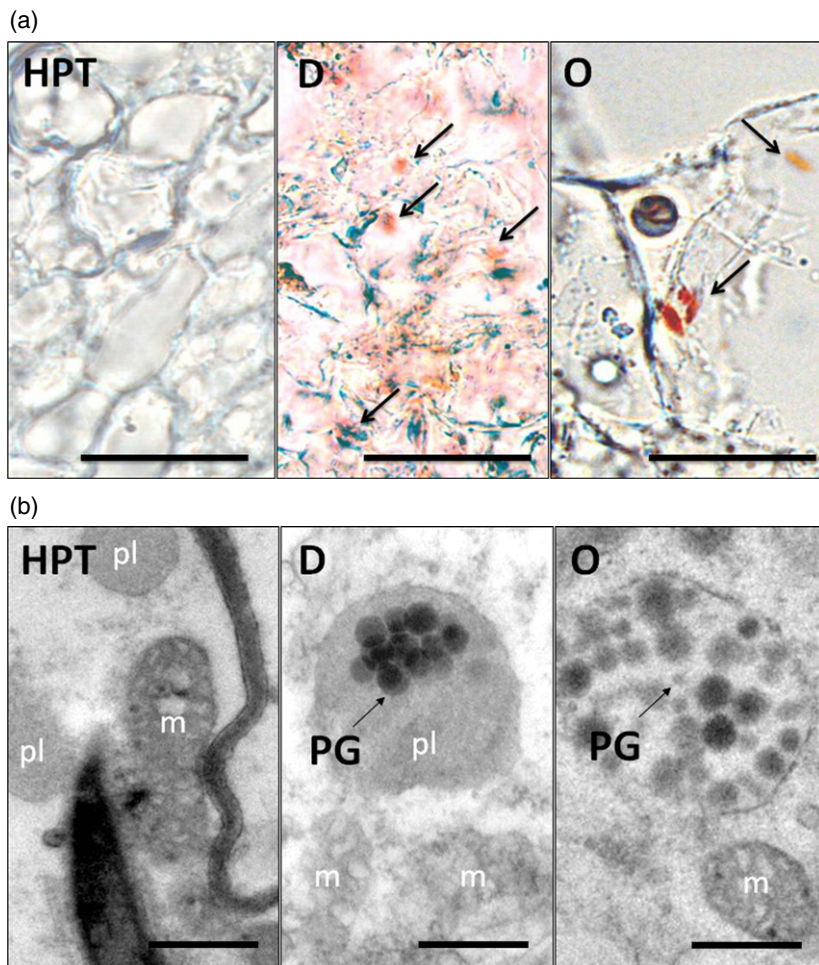


Figure 4. Microscopic cytological analysis of transgenic rice callus.

(a) Light micrographs of transgenic rice callus expressing *HPT* (HPT), transgenic rice callus expressing *ZmPSY1*, *PaCRT1* and *AtDXS* (D), and transgenic rice callus expressing *ZmPSY1*, *PaCRT1* and *AtOR* (O). Arrows indicate orange carotenoid crystal-like structures. Scale bars = 20 μm .

(b) Transmission electron micrographs of transgenic rice callus expressing *HPT* (HPT), transgenic rice callus expressing *ZmPSY1*, *PaCRT1* and *AtDXS* (D), and transgenic rice callus expressing *ZmPSY1*, *PaCRT1* and *AtOR* (O). Arrows indicate pigment-containing plastoglobuli (PG) in the chromoplast. Scale bars = 1 μm . pl, plastid; m, mitochondria.

analysis of multiple genes and their interactions over much shorter experimental time scales than possible in maize. Similar to white maize endosperm, rice callus is also white and does not accumulate significant levels of carotenoids. In addition, as a relatively undifferentiated tissue, it is likely that rice callus also lacks significant components of most of the complex secondary pathways found in plants, suggesting it may be used as a platform to test many aspects of secondary metabolism.

Although we anticipated the need to test transgenes using constitutive promoters suitable for undifferentiated tissues, we found that each of the endosperm-specific promoters that we used for the maize platform was also active in rice callus tissue, as revealed by growth of callus with a range of yellow, orange or pink hues depending on the transgene complement, showing that carotenoids were synthesized. The promiscuous activity of endosperm-specific promoters has been reported previously, e.g. Wu and Messing (2009) showed that a maize 27 kDa γ -zein promoter was sufficient to drive high-level expression of GFP in maize callus (the endogenous γ -zein protein also accumulated in the callus), and suggested that the tissue

specificity of storage proteins was a more recent evolutionary event and that older storage protein genes were less restricted. By confirming the activity of four endosperm-specific promoters in the callus of a heterologous plant species, our data suggest that rice callus may be used as a platform to test transgene expression and activity in the endosperm without the need to generate mature, seed-bearing transgenic plants, therefore providing a rapid screening platform that avoids the labor-intensive process of regeneration and breeding.

The rice callus platform reveals multiple bottlenecks in the carotenoid biosynthesis pathway

One of the most important attributes of the combinatorial transformation system, either in seed endosperm or dedifferentiated embryo-derived callus, is its ability to reveal multiple bottlenecks in metabolic pathways. Traditionally, metabolic engineering has involved a trial-and-error approach in which elimination of one bottleneck merely serves to reveal the next bottleneck, and many experiments are required to identify the most suitable engineering strategy. In contrast, combinatorial transformation

generates a library of metabolic variants allowing the best strategy to be deduced in a single step if all necessary combinations of transgenes are represented in the population (Zhu *et al.*, 2008, 2013; Naqvi *et al.*, 2010; Bai *et al.*, 2011). Here, we established that rice callus expressing the *ZmPSY1* gene was pale yellow and accumulated 17-fold more total carotenoids than control callus, but addition of *AtDXS* boosted the accumulation of carotenoids by a further 1.8-fold, resulting in a darker yellow color compared to callus expressing *ZmPSY1* alone. Similarly, callus expressing both *ZmPSY1* and *PaCRTI* was yellow/orange in color, but addition of *AtDXS* generated orange callus that accumulated twice the amount of total carotenoids compared to callus expressing only the two transgenes.

These data suggest that DXS eliminates a bottleneck in the supply of precursors to the carotenoid pathway, increasing the overall flux. In previous studies, analysis of transgenic plants expressing DXS revealed higher levels of diverse isoprenoids, including chlorophylls, tocopherols, carotenoids, abscisic acid and gibberellic acid, showing that DXS is a rate-limiting enzyme in production of plastid-derived isopentenyl diphosphate (Estevez *et al.*, 2001). Expression of *A. thaliana* DXS in tomato fruits (*Solanum lycopersicum*) increased the carotenoid content 1.6-fold (Enfissi *et al.*, 2005), and expression of *Escherichia coli* DXS in potato tubers (*Solanum tuberosum*) increased the carotenoid content twofold (Morris *et al.*, 2006). The combined data from our callus experiments and the transgenic plants discussed above suggest that enough DXS is normally produced to provide 50% of the maximum potential flux into the carotenoid biosynthesis pathway, but expressing a DXS transgene boosts the flux to the maximum capacity of the carotenoid pathway in the absence of further augmentation, resulting in a doubling of total carotenoid levels in several species. Hence rice callus expressing *ZmPSY1* alone produces $84.9 \pm 4.3 \mu\text{g g}^{-1}$ dry weight total carotenoids, whereas expression of both *ZmPSY1* and *AtDXS* doubles the flux and the callus produces $144.8 \pm 19.6 \mu\text{g g}^{-1}$ dry weight total carotenoids.

Our mathematical model suggests the flux channel for phytoene production is approximately twice as strong when *AtDXS* is introduced, as may be seen by comparing the *k1* values for the callus line expressing *AtDXS* and *ZmPSY1* with the *k1* values for the callus line expressing only *ZmPSY1* (Table S4). This indicates that phytoene production is a limiting factor for carotenoid biosynthesis, and that *AtDXS* removes this bottleneck by increasing the availability of precursors.

The *CRTI* gene product catalyzes the entire desaturation sequence from 15-*cis*-phytoene to all-*trans*-lycopene, thus spanning the rice desaturation reactions. It has been previously shown that *CRTI* replaces the function of inhibited desaturases (Misawa *et al.*, 1993). When *PaCRTI* is introduced to the tobacco, the amounts of α - and β -carotene

increase. Our parameter estimation results are consistent with this enzyme increasing the flux capacity of the callus desaturase system per unit time sixfold, as may be seen by comparing the *k2* + *k4* values in lines expressing *PaCRTI* with the *k2* values for callus lines lacking this gene (Table S4). The capacity for α -carotene synthesis is also increased by more than threefold, as may be seen by comparing the *k3* + *k5* values in the lines expressing *PaCRTI* with the *k3* values for the callus lines lacking this gene (Table S4). The lines expressing *PaCRTI* are predicted to increase flux per unit time towards production of carotenoids. This may be seen by comparing the *k1* values in lines expressing and lacking *PaCRTI* (i.e. PSY versus PSY-CRTI and PSY-DXS versus PSY-CRTI-DXS). This result is consistent with a system in which conversion of phytoene into other carotenoid precursors limits production of those carotenoids.

The rice callus platform allows functional characterization of uncharacterized genes involved in carotenoid biosynthesis and accumulation

Having established the investigative value of the callus platform by testing it using a combinatorial panel of well-characterized carotenogenic genes, we next investigated the functions of genes that are absent in plants but may extend plant β -carotene and zeaxanthin biosynthesis pathways to astaxanthin biosynthesis pathway in rice, using a synthetic *C. reinhardtii* β -carotene ketolase (*sCrBKT*) gene optimized for maize codon usage. We co-transformed rice callus with *sCrBKT* plus *ZmPSY1* and *PaCRTI*, as these genes are required to establish the early part of the pathway and provide the necessary intermediates for ketolation. It was easy to identify the callus expressing *sCrBKT*, *ZmPSY1* and *PaCRTI* because accumulation of ketocarotenoids was indicated by a pink color. Ketocarotenoids represented 25–42% of total carotenoids in these lines, predominantly astaxanthin plus lower amounts of adonixanthin, adonirubin, canthaxanthin, 3-hydroxyechinenone and echinenone. Use of the callus system therefore confirmed that the optimized synthetic gene was expressed in plants, that the enzyme was active and cooperated with endogenous carotenogenic enzymes, and that the activity of *sCrBKT* depended on concurrent activity of *ZmPSY1* and *PaCRTI*, as expected.

In plants, carotenoids accumulate in specialized pigment-bearing structures known as plastoglobuli, within plastid-derived organelles called chromoplasts (Vothknecht and Soll, 2005; Brehelin *et al.*, 2007). The cauliflower *Orange* (*OR*) gene was discovered following analysis of a mutant cauliflower with an orange curd, and was shown to encode a chaperone-like protein that induced formation of chromoplasts and thus created a metabolic sink for carotenoids (Lu *et al.*, 2006; Li and Van Eck, 2007).

Orthologs of cauliflower wild-type *OR* have been identified in other species, but only the sweet potato ortholog

has been shown to induce carotenoid accumulation (Kim *et al.*, 2013b). We therefore cloned the *A. thaliana OR* gene and found that the corresponding protein was 74.4% identical to the cauliflower wild-type ortholog and contained the DnaJ cysteine-rich domain, which is required for chaperone activity (Miernyk, 2001). Over-expression of *AtOR* increased the level of total carotenoids by twofold. Interestingly, the wild-type cauliflower *OR* allele did not increase carotenoid levels when it was expressed in potato, whereas the originally discovered mutant allele increased β -carotene levels in the tubers by sixfold, suggesting that the mutation caused a dominant gain of function (Lu *et al.*, 2006; Lopez *et al.*, 2008). It is unclear why the wild-type cauliflower *OR* allele was unable to increase carotenoid levels in potato tubers whereas the wild-type sweet potato gene was able to induce carotenoid accumulation in sweet potato callus (Kim *et al.*, 2013b) and the wild-type *A. thaliana* gene was able to increase carotenoid levels in rice callus (this study). The lack of carotenoid accumulation observed in transgenic potatoes may reflect the analysis of only four lines, which may have been subject to silencing (Lu *et al.*, 2006). Further experiments are required to identify and characterize proteins that associate with *OR*, in order to determine its precise role in chromoplast differentiation and carotenoid accumulation.

Carotenoid–lipoprotein structures may be induced either by *OR* gene expression or enhanced accumulation of carotenoids in the absence of *OR*

Chromoplasts are typically found in mature storage tissues, and are categorized as globular, tubular, reticulotubular, membranous or crystalline sub-types (Sitte *et al.*, 1980). For example, crystalline bodies have been observed in carrots (*Daucus carota*; Frey-Wyssling and Schwegler, 1965) and tomatoes (Harris and Spurr, 1969). We analyzed the structure and ultrastructure of rice callus expressing the *A. thaliana OR* gene, and observed one or two typical orange chromoplast structures per cell, as previously described in mutant cauliflower and transgenic potato tubers expressing the dominant cauliflower *OR* allele (Lu *et al.*, 2006; Lopez *et al.*, 2008). We assumed that ectopic chromoplasts were formed because the *OR* transgene induced precocious differentiation of these structures from immature plastids. However, we also observed chromoplast-like structures in callus expressing *AtDXS*, *ZmPSY1* and *PaCRT1*, but not in callus expressing *ZmPSY1* and *PaCRT1*. These data suggest that chromoplast differentiation may be triggered either by direct expression of a gene involved in the differentiation process (*OR*) or by increasing the flux through the carotenoid pathway to such an extent that the process of chromoplast differentiation is triggered by the abundance of carotenoids. This phenomenon has previously been observed in non-green *A. thaliana* tissues (callus and roots) expressing high levels of phytoene

synthase (Maass *et al.*, 2009), suggesting that the chromoplast differentiation program may be a response to accumulation of carotenoids above a certain threshold unless it is triggered by *OR* before this threshold is reached (Maass *et al.*, 2009). There appears to be no relationship between these independent events, because the *OR* gene does not normally induce the activity of carotenogenic genes (Li *et al.*, 2001, 2006), thus suggesting that it may act at the level of the metabolome by shifting the chemical equilibrium in the cell towards carotenogenesis (Li *et al.*, 2001; Maass *et al.*, 2009). More recently, sweet potato *OR* was shown to induce carotenogenic gene expression, suggesting that *OR* may contribute towards increasing carotenoid levels to reach the threshold necessary to trigger chromoplast differentiation (Kim *et al.*, 2013b).

CONCLUSIONS

Our callus-based assay allows the rapid combinatorial testing of various expression constructs, making it an ideal platform for synthetic biology, which involves assembly of genetic circuits from components such as promoters, genes and protein targeting signals. The callus platform allows large numbers of constructs to be tested in parallel, in various combinations, so that ideal engineering strategies may be developed before any transgenic plants are produced. Similarly, the platform may be used to modulate promoter strength, protein synthesis and metabolite production, thus facilitating a more quantitative approach to synthetic biology and thus more refined and sophisticated strategies for metabolic engineering. The method is applicable to any pathway and any gene product that may be analyzed through standard analytical procedures such as HPLC, MS, NMR, etc. It is neither limited nor constrained by a color phenotype.

EXPERIMENTAL PROCEDURES

Gene cloning and vector construction

The *AtDXS* and *AtOR* cDNAs were cloned directly from *A. thaliana* mRNA by RT-PCR based on sequence data in GenBank (accession numbers NM203246 and U27099.1, respectively). The cDNAs were transferred to the pGEM-T Easy vector (Promega, www.promega.com), and the resulting plasmids pGEM-*AtDXS* and pGEM-*AtOR* were digested with *EcoRI*. *AtDXS* was introduced into vector pRP5 (Su *et al.*, 2001), containing the rice prolamin promoter and the ADPGPP terminator, whereas *AtOR* was introduced into vector p326 (Stoger *et al.*, 1999), containing the wheat low-molecular-weight glutenin gene promoter and the *nos* terminator.

A truncated β -carotene ketolase gene from *C. reinhardtii* (Zhong *et al.*, 2011) was chemically synthesized and optimized for maize codon usage. The modified gene (*sCrBKT*) was fused with the transit peptide sequence from the *Phaseolus vulgaris* small subunit of ribulose biphosphate carboxylase (Schreier *et al.*, 1985) and the 5' UTR of the rice alcohol dehydrogenase gene (Sugio *et al.*, 2008) under the control of the maize γ -zein promoter. The transit peptide sequence and 5' UTR were also optimized for maize codon usage.

The maize *PSY1* cDNA was cloned from maize inbred line B73 by RT-PCR using forward primer 5'-AGGATCCATGGCCATCATAC TCGTACGAG-3' and reverse primer 5'-AGAATTCTAGGTCTGGCCA TTTCTCAATG-3' based on the *PSY1* sequence (GenBank accession number AY324431). The product was transferred to pGEM-T Easy (Promega) for sequencing, and then to the p326 vector containing the LWM glutenin promoter and *nos* terminator (Stoger *et al.*, 1999).

The *Pantoea ananatis* (formerly *Erwinia uredovora*) *CRTI* gene was fused in-frame with the transit peptide sequence from the *P. vulgaris* small subunit of ribulose biphosphate carboxylase (Schreier *et al.*, 1985) in plasmid pYPIET4 (Misawa *et al.*, 1993), and amplified by PCR using forward primer 5'-ATCTAGAATGGCT TCTATGATATCCTCTTC-3' and reverse primer 5'-AGAATTCTCAA TCAGATCCTCCAGCATCA-3'. The product was transferred to pGEM-T Easy for sequencing, and then to pHorp-P (Sorensen *et al.*, 1996) containing the barley δ -hordein promoter and the rice ADPGPP terminator. All transformation constructs were verified by sequencing.

Rice transformation

Seven-day-old mature rice zygotic embryos were bombarded with 10 mg gold particles coated with the carotenogenic constructs and the selectable maker *HPT* at a ratio 3:1 as previously described (Christou *et al.*, 1991). The embryos were returned to osmoticum medium contains MS medium supplemented with 0.3 g/l casein hydrolysate, 0.5g/l proline and 72.8 g/l mannitol for 12 h before selection on medium supplemented with 50 mg L⁻¹ hygromycin and 2.5 mg L⁻¹ 2,4-dichlorophenoxyacetic acid in the dark for 2–3 weeks (Christou, 1997). Callus was selected by visual screening for yellow, orange and pink coloring as appropriate, and was sub-cultured every 2 weeks to collect sufficient material for further analysis.

Analysis of mRNA

We separated 30 μ g of denatured RNA by 1.2% w/v agarose/formaldehyde gel electrophoresis in 1 \times MOPS buffer, and transferred the fractionated RNA to a membrane by capillary blotting (Sambrook *et al.*, 1989). The procedures described by Zhu *et al.* (2008) were used. The forward and reverse primers for each transgene are shown in Table S5.

Carotenoid extraction and quantification

Carotenoids were extracted from 10 mg freeze-dried callus in the dark using 50/50 v/v tetrahydrofuran and methanol at 60°C for 20 min. The mixture was filtered, and the residue was re-extracted in acetone. Lutein and zeaxanthin were separated on a YMC C30 carotenoid HPLC column (particle size (μ m): 3 μ m; length (mm): 100mm; internal diameter (mm):2.0 mm; Waters, <http://www.waters.com>) using a mobile phase comprising solvent A (methanol:water, 80:20 v/v) and solvent B (100% *tert*-butylmethylether) at a flow rate of 0.30 ml min⁻¹. All other carotenoids were separated on a reversed-phase ACQUITY UPL BEH 300 Å C18 column (particle size (μ m): 1.7 μ m, length (mm): 150 mm, internal diameter (mm):2.1 mm; Waters) using a gradient system with the mobile phase consisting of solvent A (acetonitrile/methanol, 70:30 v/v) and solvent B (100% water) at a flow rate of 0.35 ml min⁻¹. The mixtures were analyzed using an ACQUITY Ultra Performance LC system (Waters) linked to a 2996 photo diode array detector (Waters). MassLynx software version 4.1 (Waters) was used to control the instruments, and for data acquisition and processing (Rivera *et al.*, 2013).

Microscopy

Rice callus pieces (0.5 \times 2.0 mm) were fixed in 2.5% v/v glutaraldehyde and 2.0% v/v paraformaldehyde in 0.1 M sodium phosphate buffer (pH 7.2) overnight at 4°C for light and transmission electron microscopy. After three washes (10 min each) with 0.1 M sodium phosphate buffer (pH 7.2) at room temperature, they were sectioned on a Leica CM3050 (<http://www.leica-microsystems.com>) cryotome using CryoGel™ (High Viscosity Water Soluble Media for Frozen Sections, <http://www.2spi.com/catalog/chem/cryogel.shtml>) as the embedding medium for light microscopy. Thin sections (16 μ m) were prepared with a diamond knife using a Reichert-Jung Ultramicrotome Ultracut E (Nova Scotia, <http://www.leica-microsystems.com>), and were mounted on glass slides for analysis under a Zeiss Axioplan light microscope (<http://www.zeiss.com>) coupled to a Leica DC 200 digital camera.

For transmission electron microscopy, the sections were washed three times in 0.1 M sodium phosphate buffer (pH 7.2), and post-fixed in 1% w/v osmium tetroxide in 0.1 M sodium phosphate buffer (pH 7.2) for 1 h. They were then washed three times in re-distilled water and dehydrated in an alcohol series (30–100%) before embedding in epoxy resin Araldite® Embed 812 (Epon-812) from Aname Electron Microscopy Sciences, Madrid, Spain (URL: www.aname.es) and polymerizing at 60°C. Ultra-thin sections (80–90 nm) were prepared with a diamond knife using a Reichert Jung Ultramicrotome Ultracut E (Scotia), mounted on SPI-Chem™ Formvar®/carbon-coated copper grids, and stained with uranyl acetate and Reynold's lead citrate prior to examination using an EM 910 transmission electron microscope (Zeiss).

Mathematical modeling

Mathematica (Wolfram, 1999) was used to create and solve the mathematical models for carotenoid biosynthesis. It was also used to find the best-fit parameters for the models. Further details about the modeling process are provided in Method S1.

ACKNOWLEDGEMENTS

This study was supported by the Ministerio de Ciencia e Innovación, Spain (AGL2010-15691, BFU2010-17704 and BIO2011-22525), the Generalitat de Catalunya (2009SGR809), and a European Research Council Advanced Grant (BIOFORCE). We thank Veronica Teixido and Jorge Comas (Department Ciències Mèdiques Bàsiques, Universitat de Lleida & Institut de Recerca Biomèdica de Lleida Edifici Recerca Biomèdica I, Avenida Alcalde Rovira Roure 80, 25198 Lleida, Spain) for assistance with the ImageJ analysis.

SUPPORTING INFORMATION

Additional Supporting Information may be found in the online version of this article.

Figure S1. Astaxanthin biosynthesis pathway.

Figure S2. Carotenoid profiles in transgenic rice callus.

Figure S3. Simplified representation of carotene biosynthesis in transgenic rice callus lines.

Figure S4. Electron micrographs of ultra-thin sections of rice callus expressing *ZmPSY1*, *PaCRTI* and *AtOR*.

Table S1. Carotenoid content and composition in transgenic rice callus expressing *ZmPSY1* and/or *PaCRTI* and *AtDXS/AtOR*, or *ZmPSY1*, *PaCRTI* and *sCrBKT*.

Table S2. Relative amounts of mRNA expressed in the transformed rice callus lines.

Table S3. Quantification of metabolites in the various transgenic rice callus lines.

Table S4. Parameter estimation for the various rice callus lines.

Table S5. Oligonucleotide sequences of forward and reverse primers for mRNA blot analysis.

Method S1. Mathematical models for the callus lines transformed with *ZmPSY1* and/or *PaCRT1* and/or *AtDXS*.

REFERENCES

- Bai, C., Twyman, R.M., Farre, G., Sanahuja, G., Christou, P., Capell, T. and Zhu, C. (2011) A golden era – pro-vitamin A enhancement in diverse crops. *In Vitro Cell. Dev. Biol.* **47**, 205–221.
- Brehelin, C., Kessler, F. and van Wijk, K.J. (2007) Plastoglobules: versatile lipoprotein particles in plastids. *Trends Plant Sci.* **12**, 260–266.
- Capell, T. and Christou, P. (2004) Progress in plant metabolic engineering. *Curr. Opin. Biotechnol.* **15**, 148–154.
- Christou, P. (1997) Rice transformation by bombardment. *Plant Mol. Biol.* **35**, 197–203.
- Christou, P., Ford, T.L. and Kofron, M. (1991) Production of transgenic rice (*Oryza sativa* L.) plants from agronomically important indica and japonica varieties via electric discharge particle acceleration of exogenous DNA into immature zygotic embryos. *Biotechnology*, **9**, 957–962.
- Dafny-Yelin, M. and Tzfira, T. (2007) Delivery of multiple transgenes to plant cells. *Plant Physiol.* **145**, 1118–1128.
- Enfissi, E.M.A., Fraser, P.D., Lois, L.M., Boronat, A., Schuch, W. and Bramley, P.M. (2005) Metabolic engineering of the mevalonate and non-mevalonate isopentenyl diphosphate-forming pathways for the production of health-promoting isoprenoids in tomato. *Plant Biotechnol. J.* **3**, 17–27.
- Estevez, J.M., Cantero, A., Reindl, A., Reichler, S. and Leon, P. (2001) 1-Deoxy-D-xylulose-5-phosphate synthase, a limiting enzyme for plastidic isoprenoid biosynthesis in plants. *J. Biol. Chem.* **276**, 22901–22909.
- Farre, G., Sanahuja, G., Naqvia, S., Bai, C., Capell, T., Zhu, C. and Christou, P. (2010) Travel advice on the road to carotenoids in plants. *Plant Sci.* **179**, 28–48.
- Farre, G., Bai, C., Twyman, R.M., Capell, T., Christou, P. and Zhu, C. (2011) Nutritious crops producing multiple carotenoids – a metabolic balancing act. *Trends Plant Sci.* **16**, 532–540.
- Farre, G., Rivera, S.M., Alves, R. et al. (2013) Targeted transcriptomic and metabolic profiling reveals temporal bottlenecks in the maize carotenoid pathway that can be addressed by multigene engineering. *Plant J.* **75**, 441–455.
- Frey-Wyssling, A. and Schwegler, F. (1965) Ultrastructure of the chromoplasts in the carrot root. *J. Ultrastruct. Res.* **13**, 543–559.
- Harada, H., Fujisawa, M., Teramoto, M., Sakurai, N., Suzuki, H., Shibata, D. and Misawa, N. (2009) Simple functional analysis of key genes involved in astaxanthin biosynthesis using Arabidopsis cultured cells. *Plant Biotechnol.* **26**, 81–92.
- Harris, W.M. and Spurr, A.R. (1969) Chromoplasts of tomato fruits. II. The red tomato. *Am. J. Bot.* **56**, 380–389.
- Kim, S.H., Ahn, Y.O., Ahn, M.J., Lee, H.S. and Kwak, S.S. (2011) Down-regulation of β -carotene hydroxylase increases β -carotene and total carotenoids enhancing salt stress tolerance in transgenic cultured cells of sweetpotato. *Phytochemistry*, **74**, 69–78.
- Kim, S.H., Kim, Y.H., Ahn, Y.O., Ahn, M.J., Jeong, J.C., Lee, H.S. and Kwak, S.S. (2013a) Downregulation of the lycopene ϵ -cyclase gene increases carotenoid synthesis via the β -branch-specific pathway and enhances salt-stress tolerance in sweetpotato transgenic calli. *Physiol. Plant.* **147**, 432–442.
- Kim, S.H., Ahn, Y.O., Ahn, M.J., Jeong, J.C., Lee, H.S. and Kwak, S.S. (2013b) Cloning and characterization of an *Orange* gene that increases carotenoid accumulation and salt stress tolerance in transgenic sweetpotato cultures. *Plant Physiol. Biochem.* **70**, 445–454.
- Kurowska, M., Daszkowska-Golec, A., Gruszka, D., Marzec, M., Szurman, M., Szarejko, I. and Maluszynski, M. (2011) TILLING – a shortcut in functional genomics. *J. Appl. Genet.* **52**, 371–390.
- Li, L. and Van Eck, J. (2007) Metabolic engineering of carotenoid accumulation by creating a metabolic sink. *Transgenic Res.* **16**, 581–585.
- Li, L., Paolillo, D.J., Parthasarathy, M.V., Dimuzio, E.M. and Garvin, D.F. (2001) A novel gene mutation that confers abnormal patterns of β -carotene accumulation in cauliflower (*Brassica oleracea* var. *botrytis*). *Plant J.* **26**, 59–67.
- Li, L., Lu, S., Cosman, K.M., Earle, E.D., Garvin, D.F. and O'Neill, J. (2006) β -carotene accumulation induced by the cauliflower *Or* gene is not due to an increased capacity of biosynthesis. *Phytochemistry*, **67**, 1177–1184.
- Liu, C.G., Calin, G.A., Volinia, S. and Croce, C.M. (2008) MicroRNA expression profiling using microarrays. *Nat. Protoc.* **3**, 563–578.
- Lopez, A.B., Van Eck, J., Conlin, B.J., Paolillo, D.J., O'Neill, J. and Li, L. (2008) Effect of the cauliflower *OR* transgene on carotenoid accumulation and chromoplast formation in transgenic potato tubers. *J. Exp. Bot.* **59**, 213–223.
- Lu, S., Van Eck, J., Zhou, X. et al. (2006) The cauliflower *Or* gene encodes a DnaJ cysteine-rich domain-containing protein that mediates high levels of β -carotene accumulation. *Plant Cell*, **18**, 3594–3605.
- Maass, D., Arango, J., Wu, F., Beyer, P. and Welsch, R. (2009) Carotenoid crystal formation in Arabidopsis and carrot roots caused by increased phytoene synthase protein levels. *PLoS ONE*, **4**, e6373.
- Miernyk, J.A. (2001) The J-domain proteins of *Arabidopsis thaliana*: an unexpectedly large and diverse family of chaperones. *Cell Stress Chaperones*, **6**, 209–218.
- Misawa, N., Yamano, S., Linden, H., de Felipe, M.R., Lucas, M., Ikenaga, H. and Sandmann, G. (1993) Functional expression of the *Erwinia uredovora* carotenoid biosynthesis gene *crtI* in transgenic plants showing an increase of β -carotene biosynthesis activity and resistance to the bleaching herbicide norflurazon. *Plant J.* **4**, 833–840.
- Mlalazi, B., Welsch, R., Namanya, P., Khanna, H., Geijskes, R.J., Harrison, M.D., Harding, R., Dale, J.L. and Bateson, M. (2012) Isolation and functional characterisation of banana *phytoene synthase* genes as potential cisgenes. *Planta*, **236**, 1585–1598.
- Morris, W.L., Ducreux, L.J.M., Hedden, P., Millam, S. and Taylor, M.A. (2006) Overexpression of a bacterial 1-deoxy-D-xylulose 5-phosphate synthase gene in potato tubers perturbs the isoprenoid metabolic network: implications for the control of the tuber life cycle. *J. Exp. Bot.* **57**, 3007–3018.
- Myouga, F., Akiyama, K., Motohashi, R., Kuromori, T., Ito, T., Iizumi, H., Ryusui, R., Sakurai, T. and Shinozaki, K. (2009) The chloroplast function database: a large-scale collection of Arabidopsis Ds/Spm- or T-DNA-tagged homozygous lines for nuclear-encoded chloroplast proteins, and their systematic phenotype analysis. *Plant J.* **61**, 529–542.
- Naqvi, S., Farre, G., Sanahuja, G., Capell, T., Zhu, C. and Christou, P. (2010) When more is better: multigene engineering in plants. *Trends Plant Sci.* **15**, 48–56.
- Nikolov, M., Schmidt, C. and Urlaub, H. (2012) Quantitative mass spectrometry-based proteomics: an overview. *Methods Mol. Biol.* **893**, 85–100.
- Ozsolak, F. and Milos, P.M. (2011) RNA sequencing: advances, challenges and opportunities. *Nat. Rev. Genet.* **12**, 87–98.
- Paine, J.A., Shipton, C.A., Chaggar, S. et al. (2005) Improving the nutritional value of Golden Rice through increased pro-vitamin A content. *Nat. Biotechnol.* **23**, 482–487.
- Purkayastha, A. and Dasgupta, I. (2009) Virus-induced gene silencing: a versatile tool for discovery of gene function in plants. *Plant Physiol. Biochem.* **47**, 967–976.
- Ramessar, K., Sabalza, M., Capell, T. and Christou, P. (2008) Maize plants: an ideal production platform for effective and safe molecular pharming. *Plant Sci.* **174**, 409–419.
- Rivera, S.M., Vilaro, F., Zhu, C., Bai, C., Farre, G., Christou, P. and Canela-Garayoa, R. (2013) Fast quantitative method for the analysis of carotenoids in transgenic maize. *J. Agric. Food Chem.* **61**, 5279–5285.
- Ruiz-Sola, M.A. and Rodriguez-Concepcion, M. (2012) Carotenoid biosynthesis in Arabidopsis: a colorful pathway. *Arabidopsis Book*, **10**, e0158.
- Sambrook, J., Fritschi, E.F. and Maniatis, T. (1989) *Molecular Cloning: A Laboratory Manual*. Cold Spring Harbor, NY: Cold Spring Harbor Laboratory Press, pp. 63–70.
- Schreiber, P., Seftor, E., Schell, J. and Bohnert, H. (1985) The use of nuclear-encoded sequences to direct the light regulated synthesis and transport of a foreign protein into plant chloroplasts. *EMBO J.* **4**, 25–32.
- Sitte, P., Falk, H. and Liedvogel, B. (1980) *Chromoplasts*. Stuttgart and New York, NY: Gustav Fischer Verlag, pp. 117–148.
- Snyder, M. and Gallagher, E.G. (2009) Systems biology from a yeast omics perspective. *FEBS Lett.* **583**, 3895–3899.

- Sorensen, M.B., Muller, M., Skerritt, J. and Simpson, D.** (1996) Hordein promoter methylation and transcriptional activity in wild-type and mutant barley endosperm. *Mol. Gen. Genet.* **250**, 750–760.
- Stoger, E., Williams, S., Keen, D. and Christou, P.** (1999) Constitutive versus seed specific expression in transgenic wheat: temporal and spatial control. *Transgenic Res.* **8**, 73–82.
- Su, P.H., Yu, S.M. and Chen, C.S.** (2001) Spatial and temporal expression of a rice prolamin gene RP5 promoter in transgenic tobacco and rice. *J. Plant Physiol* **158**, 247–254.
- Sugio, T., Satoh, J., Matsuura, H., Shinmyo, A. and Kato, K.** (2008) The 5'-untranslated region of the *Oryza sativa* alcohol dehydrogenase gene functions as a translational enhancer in monocotyledonous plant cells. *J. Biosci. Bioeng.* **105**, 300–330.
- Vanegas-Espinoza, P.E., Ramos-Viveros, V., Jimenez-Aparicio, A.R., Lopez-Villegas, O., Heredia-Mira, F.J., Melendez-Martinez, A.J., Quintero-Gutierrez, A.G., Paredes-Lopez, O. and Del Villar-Martinez, A.A.** (2011) Plastid analysis of pigmented undifferentiated cells of marigold *Tagetes erecta* L. by transmission electron microscopy. *In Vitro Cell. Dev. Biol.* **47**, 596–603.
- Vothknecht, U.C. and Soll, J.** (2005) Chloroplast membrane transport: interplay of prokaryotic and eukaryotic traits. *Gene*, **354**, 99–109.
- Wolfram, S.** (1999) *The Mathematica Book*, 4th edn. Cambridge, UK: Cambridge University Press.
- Wu, Y. and Messing, J.** (2009) Tissue-specificity of storage protein genes has evolved with younger gene copies. *Maydica*, **54**, 409–415.
- Zhong, Y.J., Huang, J.C., Liu, J., Li, Y., Jiang, Y., Xu, Z.F., Sandmann, G. and Chen, F.** (2011) Functional characterization of various algal carotenoid ketolases reveals that ketolating zeaxanthin efficiently is essential for high production of astaxanthin in transgenic *Arabidopsis*. *J. Exp. Bot.* **62**, 3659–3669.
- Zhu, M.J. and Zhao, S.H.** (2007) Candidate gene identification approach: progress and challenges. *Int. J. Biol. Sci.* **3**, 420–427.
- Zhu, C., Naqvi, S., Breitenbach, J., Sandmann, G., Christou, P. and Capell, T.** (2008) Combinatorial genetic transformation generates a library of metabolic phenotypes for the carotenoid pathway in maize. *Proc. Natl Acad. Sci. U S A* **105**, 18232–18237.
- Zhu, C., Naqvi, S., Capell, T. and Christou, P.** (2009) Metabolic engineering of ketocarotenoid biosynthesis in higher plants. *Arch. Biochem. Biophys.* **483**, 182–190.
- Zhu, C., Sanahuja, G., Yuan, D. et al.** (2013) Biofortification of plants with altered antioxidant content and composition: genetic engineering strategies. *Plant Biotechnol. J.* **11**, 129–141.
- Zurbriggen, M.D., Moor, A. and Weber, W.** (2012) Plant and bacterial systems biology as platform for plant synthetic bio(techno)logy. *J. Biotechnol.* **160**, 80–90.